10/6-7-95 §8①

SLAC-PUB-95-6834

Conf-950512--87

Measurements of Longitudinal Dynamics in the SLC Damping Rings*

R.L. Holtzapple, R.H. Siemann, and C. Simopoulos
Stanford Linear Accelerator Center, Stanford University, Stanford, CA 94309 USA

I. Abstract

Measurements of longitudinal beam properties in the Stanford Linear Collider (SLC) damping rings have been made using a Hamamatsu, model N3373-02, 500-femtosecond streak camera[1]. The dependence of bunch length on current and accelerating RF voltage was measured. The energy spread dependence of current was also measured. The turbulent instability threshold for the SLC damping ring is at the current of I=1.5-2.0x10^{10} particles per bunch.

II. Data Analysis and Systematic Errors

The measurements were performed on either the SLC electron or positron damping ring when the opportunities for beam time became available. We are not aware of any differences in the performance of these rings that would affect the results.

The streak camera uses synchrotron light produced in a bend magnet to determine the longitudinal bunch distribution. The light optics is described in reference 2. Longitudinal profiles of the beam distribution are fitted to an asymmetric Gaussian function given by

$$I(z) = I_0 + I_1 \exp\left\{-\frac{1}{2}\left(\frac{(z-\bar{z})}{(1+sgn(z-\bar{z})A)\sigma}\right)^2\right\}$$

where I_0=pedestal, I_1=peak of the asymmetric Gaussian. The term $sgn(z-\bar{z})A$ is the asymmetry factor which parameterizes the shape of the asymmetric Gaussian. A chi-square minimization is performed on each streak camera picture.

The systematic errors addressed using the streak camera are: 1) dispersion in the light optics, 2) the slit width of the camera, and 3) the space charge effect at the photo cathode.

Dispersion in the glass elements of the optics can be minimized by using a narrow band interference filter. The peak spectral response of the streak camera is 500nm, and the interference filter used is centered at 500nm with a 40nm full width half maximum acceptance.

The slit width contributes to the resolution of the streak camera, by choosing 200μm or less this contribution is negligible.

To eliminate the intensity effects on the photo cathode, the multichannel plate gain was set to its maximum setting and the incident light was filtered until the bunch length measurement was stable over a range of light intensities. Figure 1 exhibits the intensity effects on bunch length measurement and in this example the light is filtered by 50% to eliminate this effect.

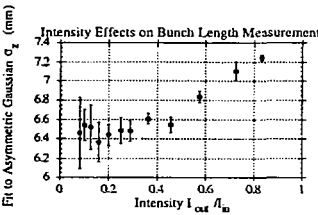

Figure 1. The bunch length dependence on light intensity measured at the damping ring with a current of I=3.6x10^{10}.

In addition, beam related background light is detrimental to the signal to noise ratio of the streak camera. A light chopper, triggered on the same beam pulse as the streak camera, is used to reduce the background to acceptable levels.

III. Single Particle Properties

A number of beam properties depend on single particle behavior. They are calculable and can be used to validate the potential of the camera. They are: 1) the longitudinal damping time, 2) the dependence of bunch length on gap voltage, and 3) the synchrotron period.

The longitudinal emittance in the damping ring damps exponentially. The bunch length versus time elapsed since injection can be used to determine the longitudinal damping time. After the beam is injected the streak camera is triggered on damping ring turn 5000 where ten measurements of the bunch length are made. Each subsequent 1000 turns the measurement is repeated until the bunch length is fully damped. The mean bunch length is computed for each time setting, and the data was fit to the function

$$\sigma^2(t) = \sigma_{eq}^2 + \exp\left(-\frac{2t}{\tau_\delta}\right)\left(\sigma_{inj}^2 - \sigma_{eq}^2\right)$$

where the points are weighted by the root mean error squared. The fitting parameters are σ_{eq} the equilibrium bunch length, σ_{inj} the injected bunch length, and the

*Work supported by the Department of Energy contract DE-AC03-76SF00515

Presented at the 16th IEEE Particle Accelerator Conference (PAC 95) and International Conference on High Energy Accelerators, Dallas, Texas, May 1-5, 1995

MASTER

longitudinal damping time τ_δ. The measured damping time for the positron damping ring is $\tau_\delta = 1.87 \pm 0.13\, msec$.

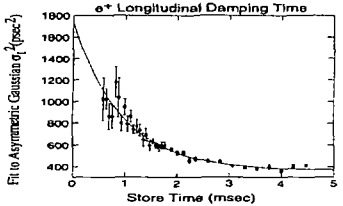

Figure 2. The longitudinal damping time in the damping ring. The solid line is a fit to the data.

The theoretical longitudinal damping time can be calculated by knowing the beam energy and magnetic field strengths of the magnets. The calculated value is $\tau_\delta = 1.79\, msec$[3] which is in agreement with the measured value.

The equilibrium (low current) bunch length in a storage ring is inversely proportional to the square root of the RF accelerating gap voltage.

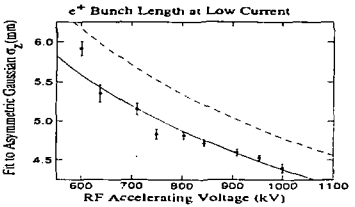

Figure 3. The equilibrium bunch length dependence on RF accelerating voltage for the damping ring at a low current of $I=0.6\times10^{10}$.

Twenty-five streak camera pictures were taken at each RF accelerating voltage. The mean and root mean error were calculated at each RF voltage setting. Fitting the data to the function $\sigma_z = A(V_{RF})^m$ gives a value of $m = -0.48 \pm 0.03$ which is in good agreement with the expected value. In figure 3 the solid line is the fit to the data and the dashed line is the expected curve based on damping ring accelerator parameters.

After injection, the bunch length oscillates in size, and fitting the bunch length to the function

$$\sigma(t) = \sigma_0 + B\sin(\Omega t + \varphi_0)$$

the synchrotron period $T_s = \frac{4\pi}{\Omega}$ can be determined. The time scale of longitudinal damping and filamentation is much longer than the 400 damping ring turns over which the measurement was performed, so they can be ignored.

The bunch length is measured 3 times every 10 turns starting at injection. The fit to the data is the solid line in figure 4. The measured synchrotron period is $T_s = 9.835 \pm 0.012\, \mu sec$ which agrees with the expected value of $T_s = 9.834\, \mu sec$.

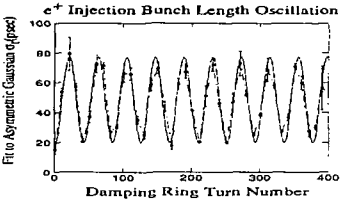

Figure 4. The bunch length oscillation in the damping ring as a function of damping ring turn number for the first 400 damping ring turns.

These results prove the usefulness of the streak camera for measuring longitudinal properties of the damping ring beam.

IV. High Current Measurements

The energy spread was measured as a function of current using a wire scanner in the transport line of the extracted beam. Given the dispersion, emittance, and beta function at the wire scanner the energy spread can be calculated from

$$\frac{\sigma_E}{E} = \frac{1}{\eta_x}\sqrt{{\sigma_{x_{wire}}}^2 - \beta_x \varepsilon_x}$$

where η_x=-0.5667m, β_x=5.41m, $\gamma\varepsilon_x$=4×10^{-5}m rad, and the energy is E=1.19GeV.

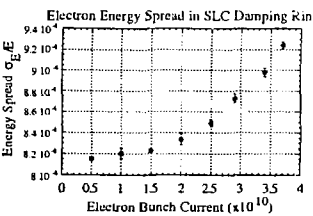

Figure 5. The energy spread as a function of current for the electron damping ring with $V_{RF} = 945\, kV$.

The measurement shows an increase in energy spread (fig. 5) at a current of I=1.5-2.0x10^{10}. This is due to the onset of a turbulent instability.

At high current the bunch length dependence on RF accelerating voltage changed due to the potential well distortion and the turbulent instability. Repeating the bunch length versus RF accelerating voltage experiment at high current and fitting the data (fig. 6) to the function $\sigma_z = A(V_{RF})^m$ gives the value of $m = -0.25 \pm 0.02$.

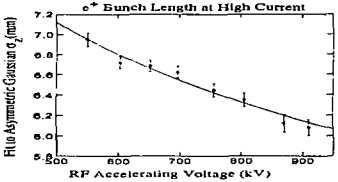

Figure 6. The bunch length dependence on RF accelerating voltage in the damping ring at a current at I=3.3x10^{10}.

The bunch length increases and the distribution changes as the current increases. This is shown in figure 7.

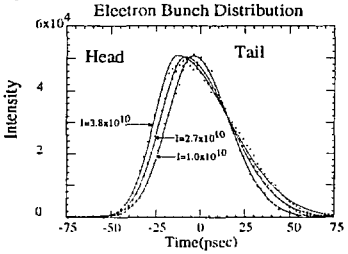

Figure 7. The bunch distribution for different currents (1.0, 2.7, and 3.8x10^{10}) in the damping rings. The plots are a sum of 25 pictures superimposed with the mean of the distributions shifted to a common origin.

Bunch length results are presented in figure 8. There is significant bunch lengthening due to potential well distortion below the turbulent threshold current of 1.5-2x10^{10}. This bunch lengthening continues above threshold

The asymmetry factor in the fitting function measures the departure from a Gaussian. Results are presented in figure 9. There is some asymmetry at low current that increases steadily due to potential well distortion. The bunch is highly asymmetric in the turbulent regime, but the dependence on current is not as strong.

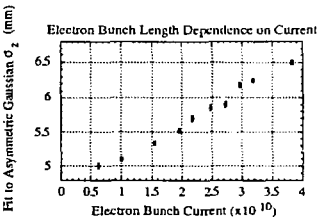

Figure 8. The bunch length dependence on current in the damping ring with $V_{RF} = 820\,kV$.

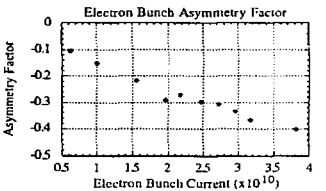

Figure 9. The asymmetry factor as function of current.

V. Conclusion

The longitudinal damping time and synchrotron tune measurement are in excellent agreement with theoretical calculations for damping rings.

The measurements of bunch length versus intensity and gap voltage provide a basis for testing our understanding of the damping ring impedance. These measurements combined with our knowledge of the impedance and other studies of the damping ring behavior serve as a guideline for the design of next generation damping rings.

The authors would like to thank K. Bane, F-J. Decker, P. Krejcik, M.. Minty, M. Ross, and J. Spencer for valuable discussions and helpful suggestions

VI. REFERENCES

[1] Hamamatsu Photonic Systems Corp., 360 Foothill Rd., Bridgewater, NJ 08807-6910.

[2] C. Simopoulos, R.L. Holtzapple, "Damping Rate Measurements in the SLC Damping Rings", SLAC-PUB-95-6813, 1995.

[3] R. Early et al., "Proposed Emittance Upgrade for the SLC Damping Rings", SLAC-PUB-6559, 1994.

DISCLAIMER